Prediction of soil water characteristic curve using artificial neural network: a new approach

Abdul-Kareem Esmat Zainal[1,*] and *Shaimaa* Hasan Fadhil[2]

[1]College of Engineering, Baghdad University, Baghdad, Iraq
[2]College of Engineering, Al-Mustansiriyah University, Baghdad, Iraq

Abstract. Soil–Water Characteristic Curve (SWCC) is an important relationship between matric suction and volumetric water content of soils especially when dealing with unsaturated soil problems, these problems may include seepage, bearing capacity, volume change, etc. where the matric or total suction may have a considerable effect on unsaturated soil properties. Obtaining an accurate SWCC for a soil could be cumbersome and sometimes it is time consuming and needs effort for some soils, either through laboratory tests or through field tests. Accurate prediction of this curve can give more precise expectations in design or analysis that include some unsaturated soil properties, which can save more effort and time. This work will concentrate on proposing a new approach for determining the SWCC using Artificial Neural Network (ANN) depending on some soil properties (air-entry point and residual degree of saturation) through computer software MatLab as a tool for ANN. The new approach is to plot the SWCC curve points instead of obtaining the parameters used in Brooks and Corey (BC) Model (1964), van Genuchten (VG) Model (1980), or Fredlund and Xing (FX) Model (1994). Results showed close agreement in determination of the SWCC by verification of the ANN results with an additional curve sample.

1 Introduction

The SWCC provides a conceptual relation between the mass (and / or volume) of water in a soil and the energy state described as (usually) matric suction of the water phase. The SWCC has proven to be an interpretive model that utilizes the capillary model to provide an understanding of the distribution of water in the voids. The effects of soil texture, void ratio, and gradation became part of the interpretation of measured laboratory SWCC data (i.e. these soil properties are used as parameters in prediction of SWCC).

The SWCCs have an important role in the determination of unsaturated soil property functions (e.g. shear strength, volume change, etc.). The procedures that have been proposed for unsaturated soil properties are approximate but satisfactory for analyzing unsaturated soil mechanics problems [1]. Neural Networks are widely used in experimental researches that need some soil parameters determination either in field or laboratory, and to describe some complex soil behavior.

2 Previous work

Many researchers had been working on using Artificial Neural Network (ANN), Genetic Programming (GP), and Genetic Based Neural Network (GBNN) in predicting the SWCC.

Lee, et al., 2005 Considered the change of void ratio during the SWCC tests. Additionally, a method reasonably predicting the SWCC for Korean weathered granite soils was suggested based on the test results obtained from the experiments conducted in their study. A method to estimate the parameters used in Fredlund and Xing's equation were proposed using an ANN (artificial neural network). The particle size distribution, compacted water content and void ratio were used as input data in the ANN model for predicting the parameters.

Johari, et al., 2006 Used Genetic-Based Neural Network (GBNN) is employed to predict the soil-water characteristic curve of unsaturated soils. A three-layer network has been trained by genetic algorithm and its topology is determined by trial and error. The network has five input neurons, namely, initial void ratio, initial gravimetric water content, logarithm of suction normalized with respect to air pressure, clay fraction and silt content.

Johari, et al., 2011 Investigated Genetic-Based Neural Network (GBNN) and Genetic Programming (GP) in determining the SWCC. These two models have identical set of input parameters. The authors utilized some soil properties as parameters to predict the SWCC, these parameters include void ratio, initial water content, clay fraction, silt content and logarithm of suction normalized with respect to air pressure. Assessment of the results indicates that predictions from GBNN model

* Corresponding author: kareem_esmat@yahoo.com

have relatively higher accuracy as compared to GP model.

Johari, and Javadi, 2011, Used a neural network which predicts the soil water characteristic curve of unsaturated soils. Their network has five input neurons, namely, initial void ratio, initial gravimetric water content, logarithm of suction normalized with respect to the atmospheric pressure, clay fraction, and silt content.

Johari, and Nejad, 2015, used Gene Expression Programming (GEP) in their research which was employed as an artificial intelligence method for modeling of the SWCC curve. The principal advantage of the GEP approach is its ability to generate powerful predictive equations without any prior assumption on the possible form of the functional relationship. GEP can operate on large quantities of data in order to capture nonlinear and complex relationships between variables of the system. The selected inputs for modeling are the initial void ratio, initial gravimetric water content, logarithm of suction normalized with respect to atmospheric air pressure, clay content, and silt content. The model output is the gravimetric water content corresponding to the assigned input suction.

Nikhil et al., 2016 Used Fredlund and Xing equation that consists of four fitting parameters. The SWCC (fitting parameters) being a function of pore size distribution and stress state vary across different sites, and thus necessitating the need for setting up a site-specific database for reasonable landslide hazard predictions under an extreme rainfall condition. Therefore, a SWCC fitting parameter estimation model has been developed via an artificial neural network (ANN) using soil samples collected from eight regions in Korea.

3 Present work

In this study, examples of ten SWCC curves were taken from experimental tests already published in literature, eight of these curves were used in the learning process of the ANN to obtain the curve points, and another two SWCC curves were used for verifying the reliability of the ANN. These curves are used just to demonstrate the proposed method; larger sets of curves may be used to obtain more accurate results that cover wider ranges of SWCC.

Depending on the typical SWCC shape as shown in Fig. 1 and 2, some ideas are discussed to express the author's point of view in determining the SWCC parameters required for the ANN.

3.1 Basic assumptions

In this work, the main difference from other solutions proposed in literature studying how SWCC were obtained is that the main factors (or parameters) that are considered herein are reduced to only two parameters, viz.:

1. The air-entry point value, where the degree of saturation is 100% and the value of Matric Suction is considered as the first input data in kPa.
2. The Sr (residual degree of saturation) point, that is considered with its value of Sr in %, and $(u_a-u_w)_r$ (Matric Suction value at Sr in kPa).

The four input data values are assumed to be the main parameters that can give a reliable SWCC points. The part of SWCC before air-entry point is considered flat, and the part of SWCC after Sr is also considered flat.

Although the SWCC vary between coarse grained soils Fig. 1 and fine grained soils Fig. 2. Since the coarse grained soils have a well-defined air entry point most of the times and a well-defined residual saturation Sr point. In fine grained soils, these points are curvy and not well-defined, the curve takes a smoother shape which leads to using extrapolation in the curve during its transient stage to obtain a defined points for air–entry and the residual stage.

In addition, the domain of the Soil Suction values are smaller for most coarse grained soils (about few hundreds kPa) and much larger for fine grained soils (up to 1×10^6 kPa).

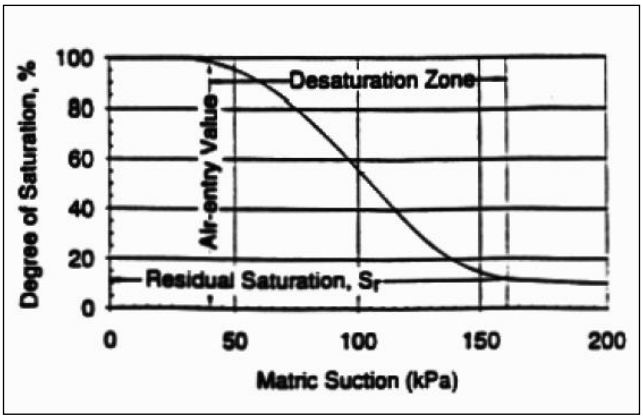

Fig. 1 Typical SWCC for most coarse grained soils [2]

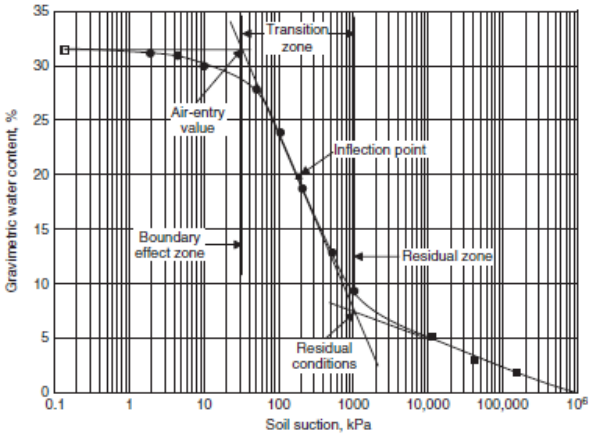

Fig. 2 Typical SWCC for most fine grained soils [1]

In this work, the air-entry point is considered as it is for coarse grained soils and for fine grained soils, it is taken as the mostly representative point near to S=100%. For coarse grained soils, the residual degree of saturation point Sr determined as the point with almost flat part at the end of the curve is considered. Where for fine grained soils, the most end flat point at the curve is considered, the purpose of this consideration is to utilize the ANN to provide the shape of the curve as it is, and the user then can define the needed points by using extrapolation.

3.2 Methodology

Ten samples of experimentally obtained SWCC were considered in this study, eight of them were used for the learning process, and the other two SWCC were used to verify the reliability of the ANN.

For each curve, the main points of the air-entry point and the Sr point is defined by their degree of saturation (S) in percent, and the Matric Suction (u_a–u_w) in kPa.

For each SWCC, the curved part between these two points (including these main points) is digitized into 21 equally spaced points (as possible) in the horizontal domain, and the values of the matric suction and the degree of saturation is obtained via a digitizing computer program (Obtaining more points give more accurate results but take more time in digitization). The two main points mentioned (with their four readings) are used as the input data to the Neural Network.

Fig. 3 shows a typical ANN where the input layer, the hidden layer(s) and the output layer are shown in sequence (A, B, C, and D symbols represent Artificial Neurons). Two networks were used to determine the SWCC. The first network has an input layer with four input neurons each represents one input value as follows:

i- Air-entry degree of saturation (in %),

ii- Air-entry Matric Suction (in kPa),

iii- Residual degree of saturation (in %), and

iv- Residual Matric Suction (in kPa).

The hidden layer will contain 20 neurons using logsig function, and the output layer will contain 21 neurons that represent the degree of saturation using purelin function.

The second network has the same input layer, this time it feeds another hidden layer with 20 neurons with logsig function, and connected to another output layer that represents the Matric Suction corresponding to the degrees of saturation obtained from the first network with 21 neurons using purelin function.

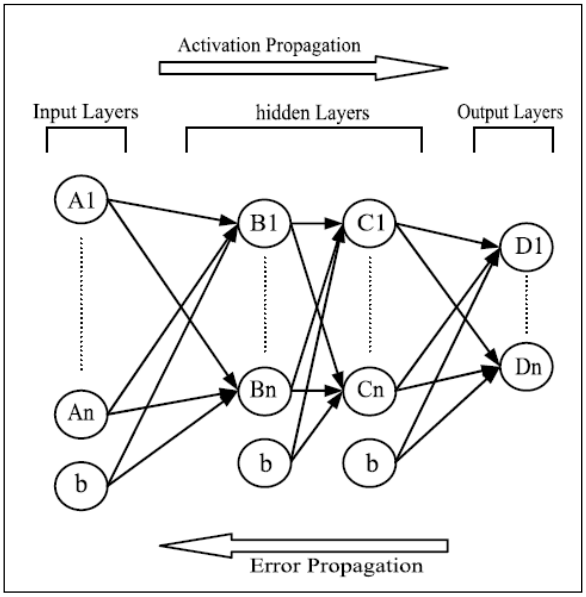

Fig. 3 Typical ANN [4]

3.3 Working procedure

The ten SWCC are shown in Fig. 4 to Fig. 9, with the reference of each one, curve 8 was taken in the training process while curves 9 and 10 were taken for the verification process.

All curves were digitized and the data obtained from digitizing these curves are illustrated in Table 1 and Table 2. Table 1 shows the values of the matric suction (u_a–u_w) in kPa for each curve, where Table 2 shows the corresponding values of the degree of saturation against each value of matric suction. The data are shown in this form as a requirement for the computer software to represent the target values. Table 3 shows the input main points for the curves (air-entry point, and the Sr point).

After the training process was complete, the two ANN (one to represent the matric suction, and the other to represent the degree of saturation) can simulate the verification data.

Results of regression for the matric suction ANN and the degree of saturation ANN are shown in Fig. 10 and Fig. 11 respectively.

The main parameters (four data points) for each curve (namely curve 9 and curve 10) was supplied to each ANN, the input data are shown in Table 4, and the results obtained are shown in Table 5.

Three curves were drawn to represent the results, the first two are the results of verifying data against the digitized data, and the third one is to represent one of the curves already used in the training process. These graphs are shown in Fig. 12, Fig. 13, and Fig. 14.

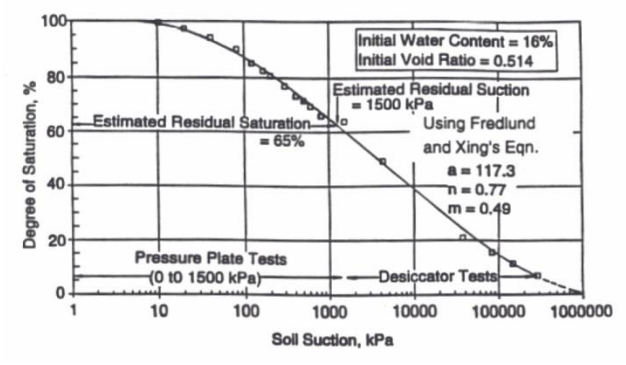

Fig. 4 SWCC for curve 1 after [2]

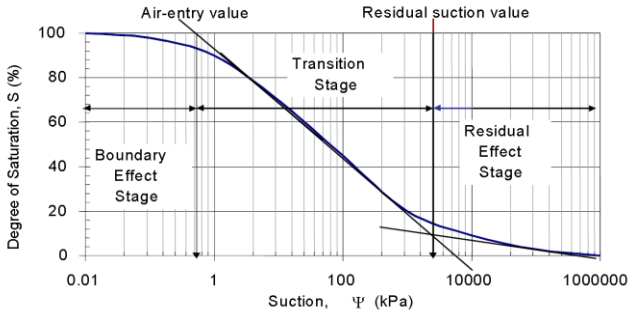

Fig. 5 SWCC for curve 2 after [13]

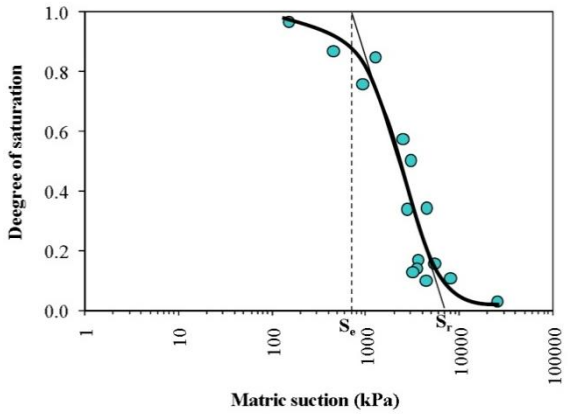

Fig. 6 SWCC for curve 3 after [11]

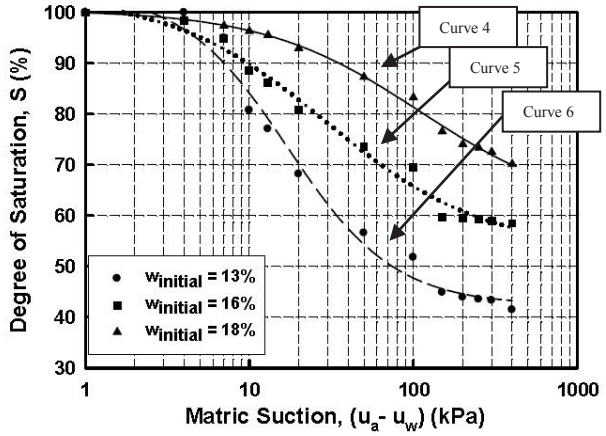

Fig. 7 SWCC for curve 4, 5, and 6 after [12]

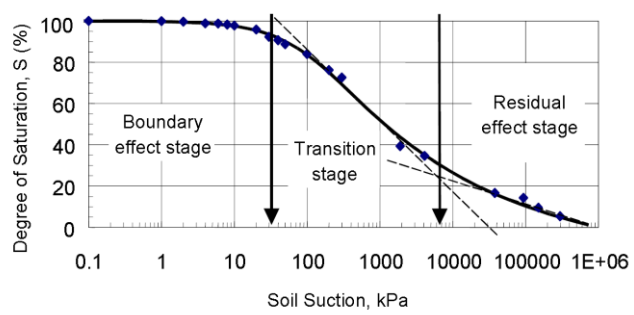

Fig. 8 SWCC for curve 7after [13]

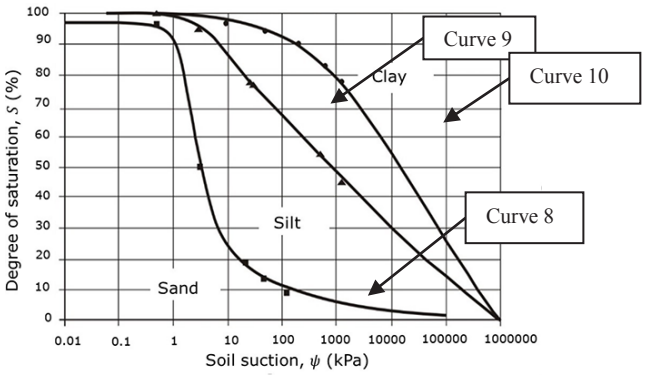

Fig. 9 SWCC for curve 8after [10]

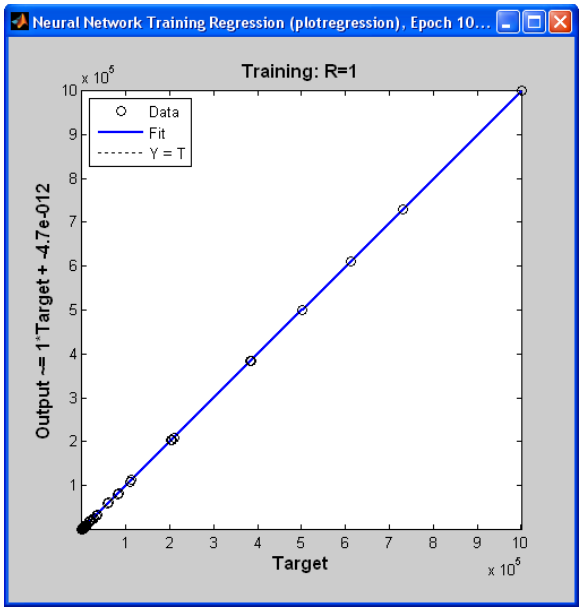

Fig. 10 the Matric Suction Regression result

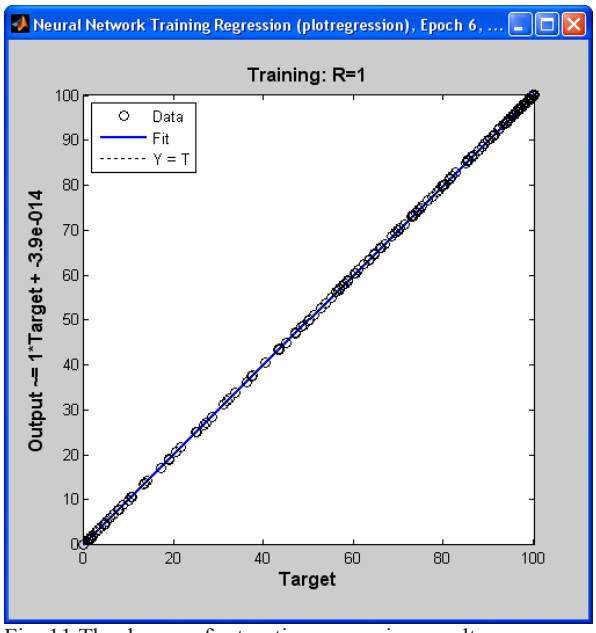

Fig. 11 The degree of saturation regression result

4 Discussion

The original curves were obtained from experimental data, the curved lines were digitized to represent the best fit for these experimental points. Results obtained and shown in Fig. 12 to Fig. 14 deviate slightly from the original curved data (as in experimental data points). The best fit lines shown are more representative in showing the curve variation.

Curve 8 best fit line can be represented by (1):

$$S = 74.14\Psi^{-(0.079+0.03536\Psi)} \quad (1)$$

with R^2=0.837

Also curve 9 best fit line can be represented by (2):

$$S = 95.12\Psi^{(0.07386-0.02383\mathrm{Ln}(\Psi))} \quad (2)$$

with R^2=0.9613

Finally, curve 10 best fit line can be represented by (3):

$$S = 104.5\Psi^{(-0.01816\Psi^{0.2011})} \quad (3)$$

with R^2=0.9736

where:

Ψ= matric suction (kPa), and

S= Degree of Saturation in percent.

The trend of these result points is the same as in the original data. It is recommended to use more curves and more data points digitized which can give more accurate curves.

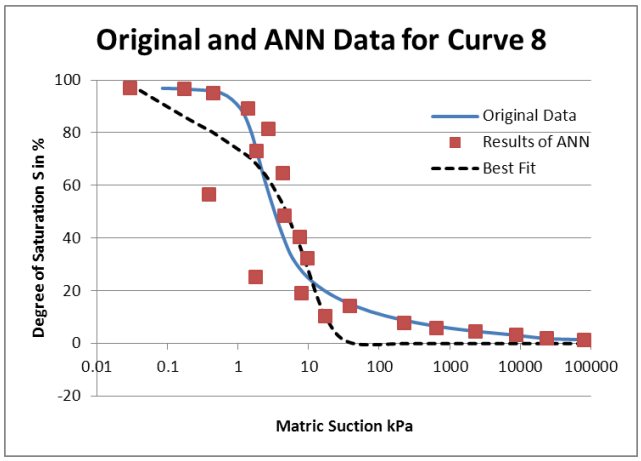

Fig. 12 Original and ANN Data for Curve 8

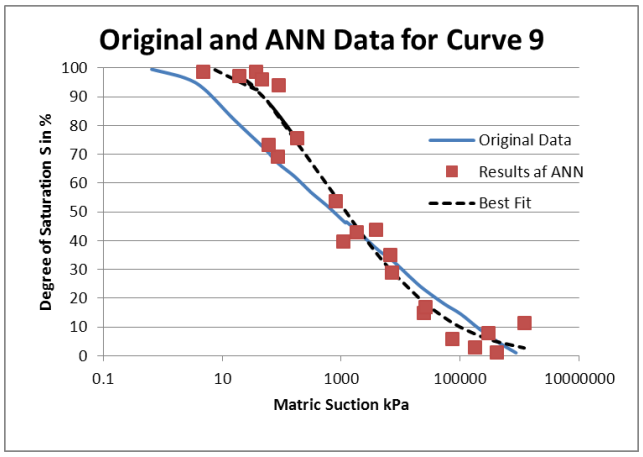

Fig. 13 Original and ANN Data for Curve 9

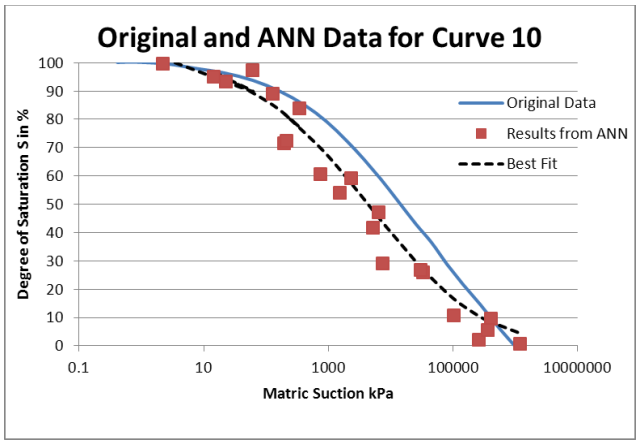

Fig. 14 Original and ANN Data for Curve 10

5 Conclusions

The new proposed method of representing the SWCC is found to be satisfactory in representing the SWCC curved segment. Further work in needed to represent the SWCC more accurately and more sample curves are needed.

Other soil properties may be included along with more representatives (i.e. void ratio, soil classification, effective diameter D10, and others).

References

[1] D. G. Fredlund, H. Rahardjo, and M. D. Fredlund, "*Unsaturated Soil Mechanics in Engineering Practice*", John Wiley & Sons, Inc. (2012).

[2] D. G. Fredlund, S. K.Vanapalli, D. E. Pufahl, "Predicting the shear strength function for unsaturated soils using the soil-water characteristic curve", Unsaturated soils : proceedings of the first International Conference on Unsaturated Soils, UNSAT '95, Paris, France, 6-8 September. Vol. **3**. (1995).

[3] A. Johari, A. Hooshmand Nejad, , "Prediction Of Soil-Water Characteristic Curve Using Gene Expression Programming", IJST, Transactions of Civil Engineering, Vol. **39**, No. C1, pp. 143-165. (2015)

[4] A. Johari, A. A. Javadi, "Prediction of soil-water characteristic curve using neural network", Unsaturated Soils – Alonso & Gens (eds) Taylor & Francis Group, London, pp. 461-466. (2011).

[5] A. Johari, G. Habibagahi, A. Ghahramani, "Prediction of a Soil-Water Characteristic Curve Using a Genetic-Based Neural Network", Scientia Iranica, Vol. **13**, No. 3, pp 284-294. (2006).

[6] A. Johari, G. Habibagahi, A. Ghahramani, "Prediction of SWCC using artificial intelligent systems: A comparative study", Scientia Iranica 8 (**5**),pp 1002–1008. (2011).

[7] S. R. Lee, Y.K. Kim, S. J. Lee, "A Method to Estimate Soil-Water Characteristic Curve For Weathered Granite Soil", Proceedings of the 16th International Conference on Soil Mechanics and Geotechnical Engineering. (2005).

[8] N.V. Nikhil, Yoon Seok, Seung-Rae Lee, Deuk-Hwan Lee, "ANN Based Estimation of SWCC Fitting Parameters for Korean Weathered Soil Considering In-Situ Characteristics", The 2016 world congress on advances on Civil, Environmental, and Materials Research. (ACEM16). (2016).

[9] Won Taek Oh, Sai K. Vanapalli, "Modelling the Stress versus Settlement Behavior of Model Footings in Saturated and Unsaturated Sandy Soils", The 12th International Conference of International Association for Computer Methods and Advances in Geomechanics (IACMAG) 1-6 October, Goa, India.(2008).

[10] N. Pérez-García, "Determination of Soil-Water Characteristic Curve with pressure plate test". in Groundwater - Contaminant and Resource Management book, Safandila, Querétaro, México: Secretaria de Comunicaciones y Transportes, Mexican Transportation Institute;. 54 p. Publicación Técnica No. 313 (in Spanish). (2008)

[11] Anuchit Uchaipichat, , "Variation of Pile Capacity in Unsaturated Clay Layer with Suction", Ejge, Vol. **17**, pp. 2425-2433. (2012).

[12] S. K ,Vanapalli, Taylan Z.N, "Design of Single Piles Using the Mechanics of Unsaturated Soils", Int. Jour. of GEOMATE, March, Vol. **(2)**, No. 1 (Sl. No. 3), pp. 197-204.(2012).

[13] S. K., Vanapalli, A. Wright, D.G. Fredlund, , "Shear Strength Behavior of a Silty Soil Over the Suction Range From 0 to 1,000,000 kPa", 53th Canadian Geotechnical Conference, at Moterial, Quebec,Canada, October. (2000).

TABLE 1. MATRIC SUCTION FOR THE 8 CURVES

1	2	3	4	5	6	7	8
8.57553	0.055602	48.1437	1.672545	1.694723	2.120678	1.434355	0.084768
21.06522	0.134151	137.1151	2.653551	2.235451	2.688841	3.182805	0.197618
32.65756	0.324312	223.0924	3.320424	2.987829	3.593593	7.78326	0.572914
62.53066	0.756323	361.177	4.617148	4.154408	5.198023	14.65592	1.07374
117.8381	1.671164	561.8744	5.6271	5.700876	6.541884	27.77551	1.485428
215.9374	3.51968	809.7844	7.134633	7.227838	8.897422	163.9119	1.838764
388.6442	7.222818	1068.71	9.410904	9.533255	10.73145	263.0179	2.228015
689.7889	14.55798	1319.747	12.25082	12.40947	12.36917	428.4782	2.746242
1212.124	28.93492	1573.873	18.62726	16.15307	15.63406	702.5664	3.428708
2117.359	56.71134	1846.009	23.68593	22.45854	20.86181	1151.982	4.373265
3683.958	110.2674	2143.724	28.52934	27.73189	26.29097	1980.802	5.922081
6422.307	218.2891	2472.965	36.11855	34.24346	32.4627	3262.017	9.679343
11218.4	421.8968	2838.589	42.37131	42.84465	40.79334	5645.563	19.59148
19596.84	1129.149	3269.114	51.56069	55.03947	46.95129	9898.265	46.6512
34436.92	2545.303	3783.747	62.65208	66.1953	56.54949	17543.03	123.0946
61363.22	5959.629	4445.367	91.29107	97.02138	80.60604	31771.46	343.3754
112443.7	14207.29	5489.569	132.4373	138.5041	107.5743	58543.65	978.5758
209809.3	34140.99	7415.32	194.6825	197.7232	164.0409	109047.6	2812.824
383060	83032.35	11011.51	254.1643	293.6675	253.8486	204000.5	8154.716
611672.6	203560.6	17446.28	313.848	387.3668	317.6452	384117	23742.62
1000000	501059.7	26079.9	403.2	478.3629	397.4737	729544.6	80976.37

TABLE 2. DEGREE OF SATURATION IN % FOR EACH CURVE

1	2	3	4	5	6	7	8
100.1479	99.16128	100	100	99.66008	100.0255	99.60786	96.87191
96.74303	97.34698	97.73097	99.09568	98.91423	99.65047	99.54323	96.50971
94.94827	95.10542	95.78695	98.90598	97.98307	97.23914	97.82207	95.09384
90.41395	91.45666	93.39106	98.34405	95.94096	93.71603	96.99501	89.29865
85.64171	86.30029	90.02373	98.15491	94.26917	90.93591	94.3787	81.36319
80.2874	79.98811	85.39129	97.59489	92.59903	86.36563	77.48374	73.0326
74.53619	73.14829	79.71971	96.47899	90.00295	82.78463	70.42706	64.73494
68.54696	66.03213	73.41563	95.46616	87.7772	80.08857	63.60235	56.56898
62.37258	58.71499	66.90828	93.95669	84.99637	74.96475	56.87706	48.46888
56.14542	51.22199	60.31059	92.38928	81.47409	69.96314	50.11863	40.40171
49.86542	43.60339	53.69032	91.19304	79.06441	64.6338	43.2609	32.4004
43.58533	36.16061	47.07007	89.9752	76.65473	61.11399	37.62905	25.12348
37.33166	28.46663	40.42723	88.53282	73.87473	57.03875	31.99731	18.96608
31.13102	19.06192	33.78439	86.82241	71.2792	55.04169	26.59754	14.12578
24.98315	14.18188	27.14154	85.46153	69.42514	52.73532	21.56227	10.50379
19.02026	10.58337	20.52125	82.0205	66.08678	48.86303	17.15659	7.869608
13.61293	7.638194	14.17199	78.49733	63.30403	47.19182	13.34738	5.893974
8.761576	5.069951	8.748892	75.34393	60.52129	44.98333	9.869533	4.445176
3.805091	2.727831	4.681239	73.28257	58.84785	43.59684	6.689906	3.259796
1.982576	1.039097	1.923897	71.24294	58.10199	43.48938	3.808504	1.909779
0	1.009049	1.674576	69.94256	57.72755	43.29969	1.324733	1.448798

TABLE 3. INPUT DATA

	1	2	3	4	5	6	7	8
ir-entry point matric suction	8.57553	0.055602	48.1437	1.672545	1.694723	2.120678	1.434355	0.084768
air-entry point S	100.1479	99.16128	100	100	99.66008	100.0255	99.60786	96.87191
Sr point matric suction	1000000	501059.7	26079.9	403.2	478.3629	397.4737	729544.6	80976.37
Sr S	0	1.009049	1.674576	69.94256	57.72755	43.29969	1.324733	1.448798

TABLE 4. VERIFYING DATA

			9	10
air-entry point matric suction			0.651432	0.410554
	air-entry point S		99.53902	100.1317
Sr point matric suction			868462.8	950007.8
		Sr S	0.987817	0.329272

TABLE 5. VERIFYING DATA RESULTS

Matric Suction kPa		Degree of Saturation S%	
9	10	9	10
4.728393	2.223661	98.71132	99.64459
36.89925	60.00188	98.6911	97.28264
19.64693	14.42446	97.28464	95.17319
46.64776	22.40805	95.88645	93.42735
88.63865	-129.106	93.829	88.91717
179.7074	345.2875	75.47142	83.76707
86.4868	197.1986	69.00925	71.41278
60.14028	210.1119	73.1	72.32742
811.1791	752.5994	53.5159	60.65005
1075.403	1510.868	39.50234	53.91856
1853.102	2333.282	42.78961	59.19435
3840.476	5252.347	43.77121	41.71416
6600.492	6502.615	35.08857	47.15224
7228.543	7531.47	28.70058	28.96275
24685.07	33397.71	14.77886	25.99016
26587.29	30670.66	16.9301	26.65161
74943.67	102013.3	5.839024	10.75616
178921.8	260958.9	2.814036	2.149345
298830.6	407437.3	7.694084	9.607634
409398.9	366794.4	0.961794	5.576248
1190123	1190970	11.33338	0.769058